VOL. 1 - No. 2 GEO International JUNE 1972

Resistivity Studies of the Imperial Valley Geothermal Area, California

T. MEIDAV * AND R. FURGERSON **

ABSTRACT

Electrical resistivity has been employed for mapping the Imperial Valley of California as part of a multi-disciplinary approach to assess its geothermal potential. Vertical and lateral resistivity changes were determined from Schlumberger depth soundings with effective probing depths up to 8000 ft.

Chief conclusions were: (1) Known geothermal anomalies appear as residual resistivity lows superimposed on the regional gradient which decreases northwestward from the southeast corner of the Imperial Valley, near the Colorado River, to values about two orders of magnitude lower at the Salton Sea. (2) A regional salinity gradient in the Imperial Valley trends northwest from a very low salinity at the Colorado River near Yuma, Arizona, to a very high salinity at the Salton Sea geothermal field. (3) Abrupt changes in salinity exist across the Imperial fault, with salinities being much higher west of the fault. (4) Maximum salinities can be estimated by combining the ground resistivity survey and formation factor-depth relationships compiled from well logs.

From a technical point of view, the apparent-resistivity and longitudinal-resistivity maps are nearly identical at a probing depth of 3000 ft. Hence continuous profiling at a Schlumberger AB/2 spacing of 3000 ft should permit an effective, low-cost reconnaissance method for still-unsurveyed areas of the Imperial Valley.

Introduction

Interest in developing geothermal energy in the Imperial Valley, California (Figure 1) has fluctuated over several decades. Previous exploitation attempts (MCNITT 1963, KOENIG 1967) were concentrated near the southern shore of the Salton Sea. These efforts were hindered by technological problems posed by very high salinity (up to 33 wt %) and high corrosiveness of the geothermal fluids. The successful development of a geothermal reservoir for power production at Cerro Prieto, Mexico, which is located in the southern extension of the Salton trough (Figure 1), provided impetus for renewed examination of the geothermal potential of the Imperial Valley. The ecological benefit derivable from a relatively non-polluting source of energy and promise of large-scale water desalination provided further incentive. As a result, investigators at the University of California, Riverside, initiated a series of geological, geophysical, and geochemical studies in the Imperial Valley (MEIDAV and REX 1970, MEIDAV 1970a, REX 1971, REX ET AL. 1971). This electrical resistivity study represents one facet of the total effort and includes data collected from 1968 to 1910.

The Imperial Valley is located approximately in the middle of the Salton trough which extends from the northern edge of the Gulf of California for about 300 km north to the San Gorgonio Pass (Figure 1). The Salton trough basin is largely filled by poorly sorted Colorado River and lacustrine sediments of Tertiary age overlain by a large thickness of Quaternary alluvium (DIBBLEE 1954). The Imperial Valley has steep margins and a stepfaulted basement at a maximum measured depth of 20,900 ft (BIEHLER, KOVACH and ALLEN 1964, BABCOCK 1969).

The Salton trough is apparently underlain by the northern extension of the East Pacific Rise (MENARD 1960), a submarine ridge extending for about 13,000 km to the south on the floor of the Pacific Ocean. The East Pacific Rise, a locus of sea-floor spreading, is characterized by abnormally high heat flows and earthquake activity (ISACKS ET AL. 1968). The high heat flows are apparently associated with the axis of two upward moving convection cells which diverge at the axis.

Near surface thermal activity in the Imperial Valley has been generally confined to boundary faults and to the Buttes area (Figure 2) where five Quaternary volcanic domes are aligned in an arc nearly normal to the Salton trough. Hot springs are the only current thermal activity, although mud pots were also observed before being submerged by the formation of the Salton Sea in 1905-1907.

* Institute of Geophysics and Planetary Physics, University of California, Riverside, California 92502. Presently with the Energy Section, Resources and Transport Division, United Nations, New York 10017, USA.

** Department of Geological Sciences, University of California, Riverside, California 92502. Presently with the Department of Geophysics, Colorado School of Mines, Golden, Colorado 80401, USA.

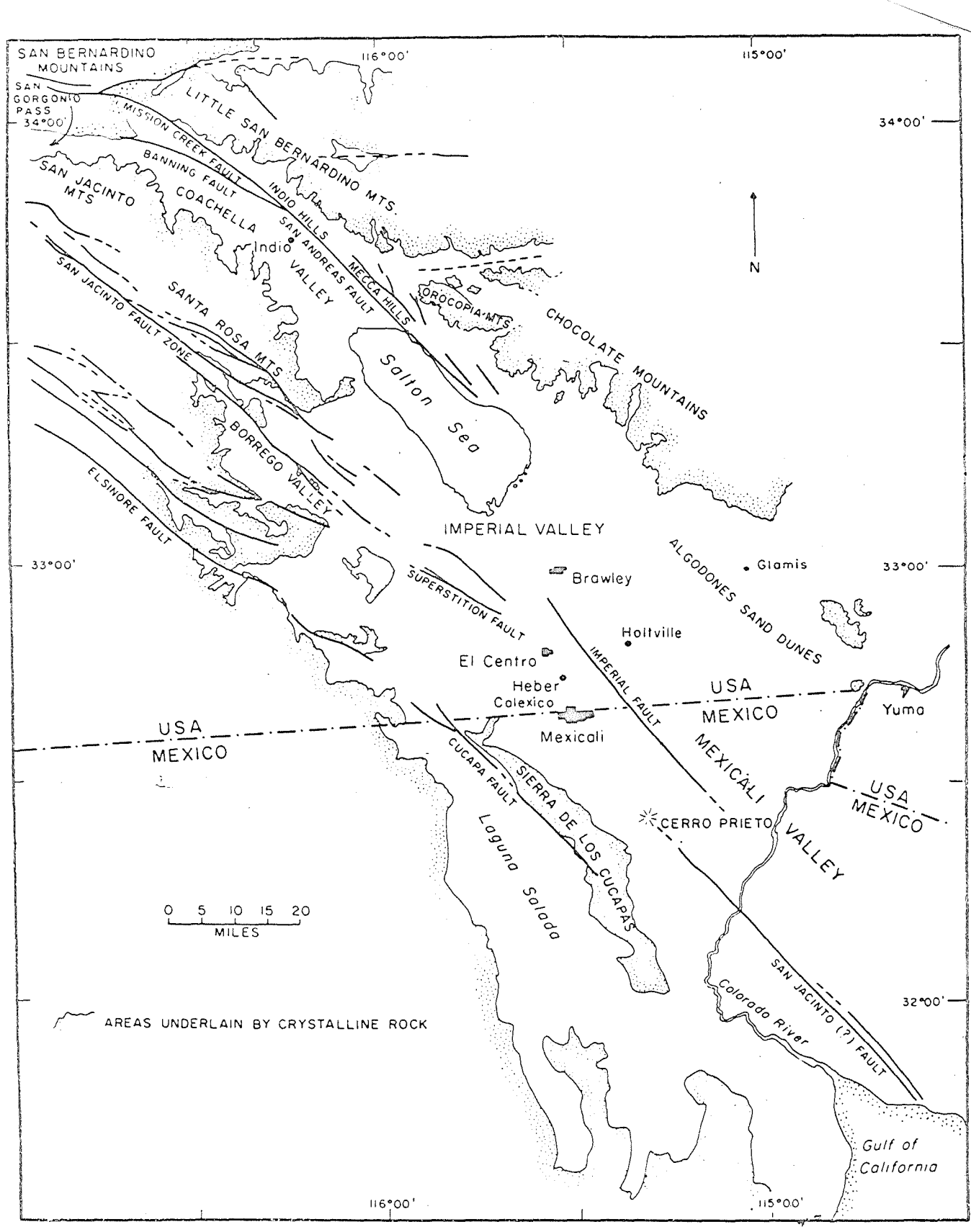

FIG. 1. — *Index map of the Salton trough which includes the Imperial Valley (after* BABCOCK 1969, BIEHLER 1964*).*

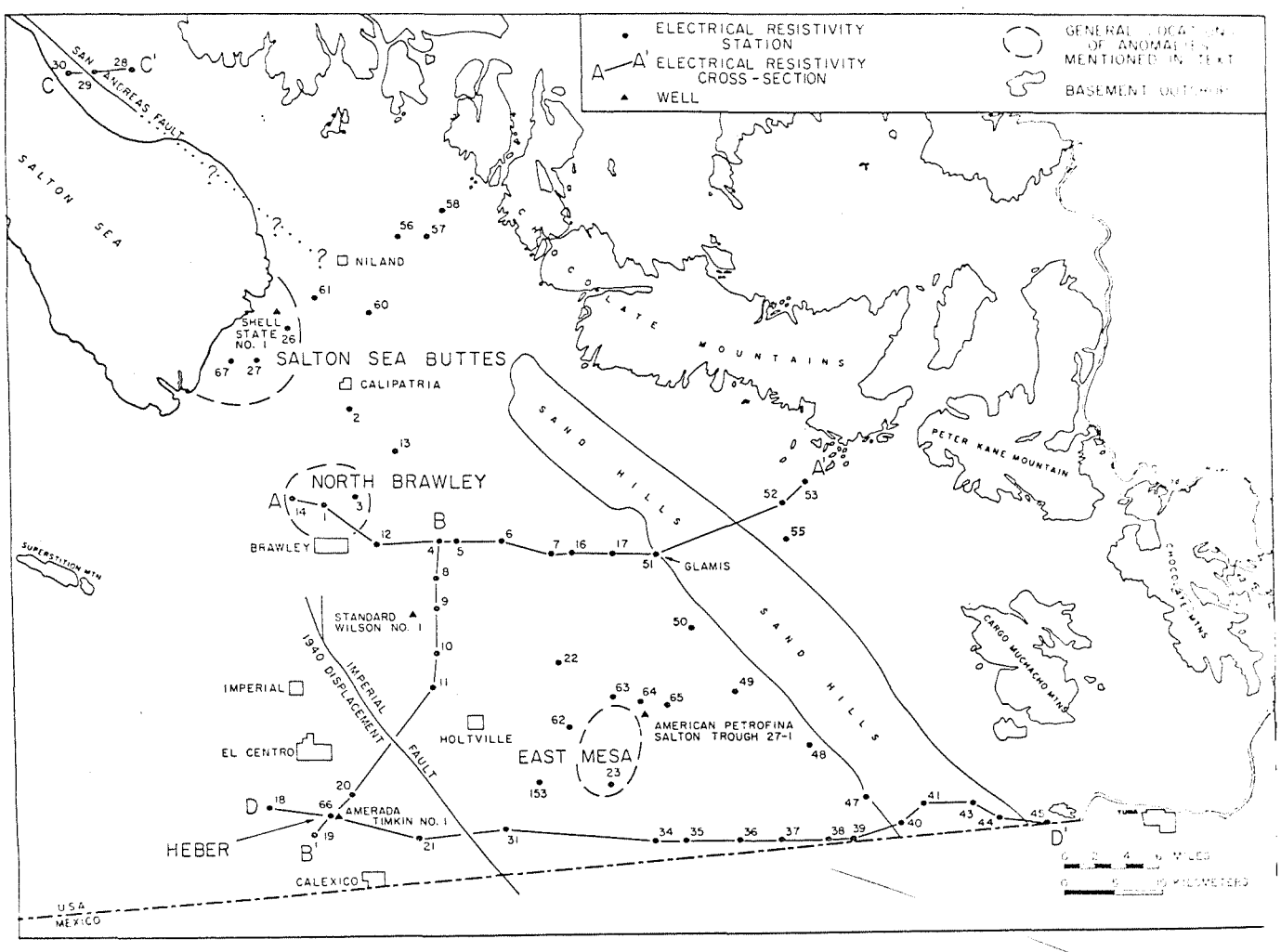

FIG. 2. — *Location map of the Imperial Valley showing resistivity stations, resistivity cross-sections, petroleum and geothermal exploration wells, and locations of the major resistivity anomalies (Buttes, North Brawley, Heber, and East Mesa).*

Previous studies

BIEHLER (1964) has continued gravity studies of the Salton trough. An unpublished aeromagnetic survey of most of the valley and its flanks was conducted by the Chevron Oil Company. A ground magnetic survey (SOSKE 1935, KELLEY 1936) and an aeromagnetic survey (GRISCOM and MUFFLER 1971) have been made of the Buttes area (Figure 2) at the south end of the Salton sea. COMBS (1971) is extending the temperature-gradient measurements began by REX (1971) and is also calculating heat flows. An unpublished salinity map of the Mexicali Valley based upon measurements to a depth of 300 m was prepared by EDUARDO PAREDES (Groundwater Division, Government of Mexico, Mexicali Branch). Extensive unpublished borehole logging was conducted by various companies in their petroleum and geothermal exploration in the Imperial Valley. Preliminary results of the 1968 electrical resistivity program were reported earlier (MEIDAV and REX 1970, MEIDAV 1970a).

Electrical resistivity in geothermal exploration

FUNDAMENTAL RELATIONSHIPS

Relationships between electrical resistivity of fluid-saturated rocks and various physical parameters which affect it have been discussed by WYLLIE (1963), KELLER and FRISCHKNECHT (1966), DAKHNOV (1962), WARD and FRASER (1967). Hence, only a brief review of the factors affecting current conduction in rocks is in order.

Current conduction in rocks other than shales and clays or metalliferous zones is, for all practical purposes, through the pore fluid. The resistivity of water-saturated rocks is given by

$$\rho_o = k\,\Phi^{-m}\rho_w = F\,\rho_w \qquad (1)$$

where

ρ_o = resistivity of the water-saturated rock
ρ_w = resistivity of the saturating electrolyte
k = a constant which usually varies from about 0.6 to 1.5
Φ = fractional porosity
m = cementation factor which usually varies from about 1.5 to 3
F = formation factor

The resistivity of a clay-free, porous rock is related (Eq. 1) to the resistivity of the saturating electrolyte (and hence to salinity), to porosity, and to the tortuosity of the mean free path of the electrical current, often termed the « cementation factor » of the rocks. MEIDAV (1970a) has constructed nomograms relating these parameters.

Increase in temperature reduces the resistivity of the electrolyte, and DAKHNOV (1962, p. 104) gives the resistivity ρ_T of a rock at a temperature T (in centigrade) containing fluid of resistivity ρ_{18} at 18 °C as

$$\rho_T = \frac{\rho_{18}}{1 + \delta\,(T - 18)} \qquad (2)$$

where δ = temperature coefficient of resistivity, usually 2.5 percent per degree centigrade. Lateral temperature changes of 100 °C and more at depth across a geothermal reservoir are not unusual. Using equation (2) a temperature change of 100 °C will reduce the resistivity to about one-fourth of that for the colder surrounding region. Hence, resistivity has been found to be a useful tool in exploration for geothermal reservoirs.

TEMPERATURE VERSUS RESISTIVITY MEASUREMENTS

In areas where the rocks overlying a geothermal reservoir are fractured and considerable non-horizontal permeability exists, fumaroles, hot springs, and high-gradient heat flow anomalies may be laterally offset from the source of heat. Furthermore, abrupt changes in geothermal gradient, including gradient reversals, are not unknown. In such cases, temperature measurements alone do not provide sufficiently reliable guides for production drilling and electrical methods may prove more reliable than thermal methods (STUDT 1958).

Where an outstanding geothermal reservoir does exist, the electrical resistivity across it usually varies by a factor of at least 3-10 (STUDT 1958, HAYAKAWA 1966, BREUSSE 1964). Because of convective circulation, the concentrating effect due to boiling, and the higher dissolving power of the heated reservoir water, the salinity of fluids within the geothermal reservoir is greater than outside the reservoir. Thus, the salinity and temperature effects are often working together to enhance the electrical conductivity of the geothermal reservoir and thus sharpen the electrical resistivity anomaly. The high contrast in resistivity between the reservoir rock and the surrounding rock is particularly notable in volcanic terrain. In such areas, the resistivity within the geothermal reservoir usually is 5 to 10 ohm-m or less, regardless of how high the resistivity is outside the reservoir area. In cases such as the present study in a deep sediment-filled valley where regional resistivity is quite low because of the large amounts of clay and shale within parts of the geological section, the resistivity contrast across a geothermal area is less outstanding. Because clay and shale possess a finite electrical conductivity of their own, they tend to attenuate the amplitude of the conductivity change due to temperature.

Instrumentation, field techniques, and interpretation procedures

In the 1968 field season, a 5-ampere Geoscience transmitter was employed as a current source. Both a Geohmite receiver and a chart recorder were used as receivers. For large electrode spacings, which required long commutation periods, the chart recorder was more efficient than the more sophisticated Geohmite receiver. In the 1970 field season a resistivity instrument designed by Chevron Oil Field Research Company was employed. Its 20 kVA capacity allowed a current load of up to 45 amperes under optimum operating conditions.

An inverse Schlumberger configuration was employed throughout the study. The term « inverse Schlumberger » refers here to an electrode array where current is injected into the ground through the internal electrodes and the potential is measured between the outer electrodes. The advantages of the inverse Schlumberger array are lower weight, lower cost, and higher safety. Because current lines are heavier than potential lines, the weight and cost of wire is considerably reduced. Shorter current lines provide for easier monitoring from the instrument truck and, therefore, for greater safety. The disadvantage of the inverse Schlumberger procedure occurs because the longer the potential electrode line, the greater is the amplitude of the telluric noise. This noise affects the quality of the data obtained at large electrode separations, and hence the maximum depth that can be reliably explored. Other considerations in the selection of the field array for this study were discussed by MEIDAV (1970b).

Square wave commutation was used throughout the study, with commutation periods from 1 to 100 seconds. Generally, the commutation period was selected by consideration of the skin depth, the depth at which the amplitude of an electromagnetic wave is reduced to $1/e$ of its surface value. If the magnetic permeability is taken to be that of free space (a valid assumption for the majority of earth materials), STACEY (1969) gives the skin depth for a homogeneous half space as

$$z = (2\pi\omega\sigma)^{-1/2} \qquad (3a)$$

in the *cgs* system where

z = skin depth
ω = angular frequency
σ = electrical conductivity.

When the frequency is too high for the depth-resistivity combination, the apparent resistivity obtained will be too high.

Another factor which may affect the accuracy of the resistivity reading is the current formation time, the time from the initiation of an electric pulse to steady-

FIG. 3.
solid

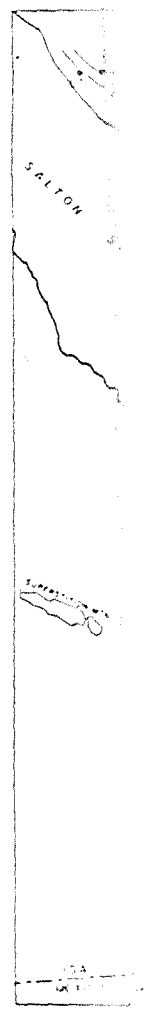

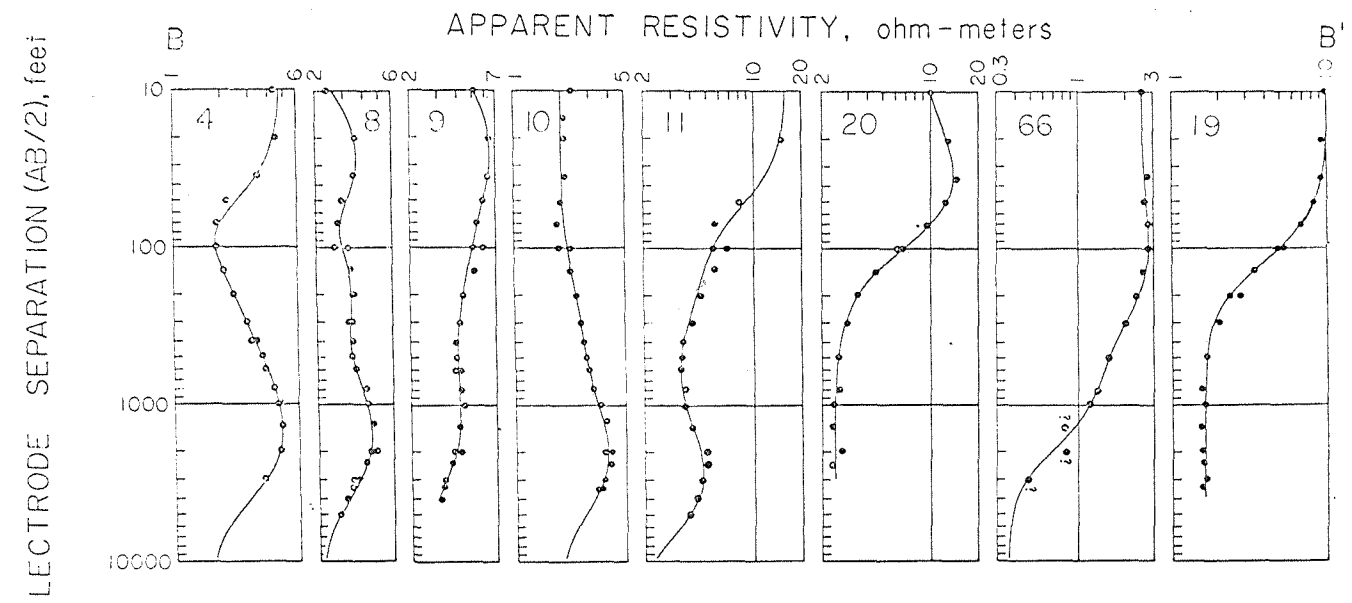

FIG. 3. — *Schlumberger resistivity soundings used to construct geoelectric cross-section B (Figure 11). Points are field data, the solid lines are computer-drawn and calculated interpretations shown in the geoelectric cross-sections.*

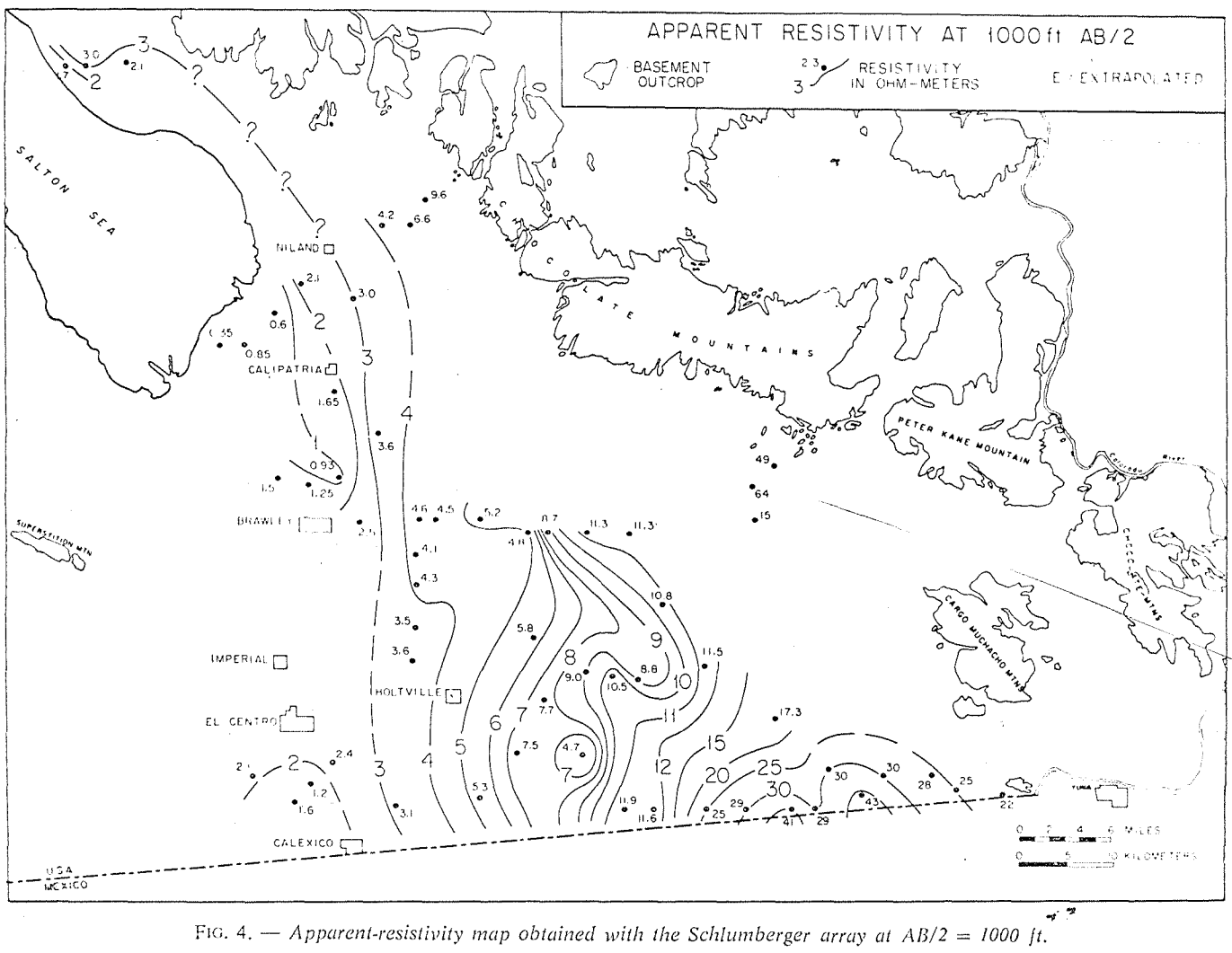

FIG. 4. — *Apparent-resistivity map obtained with the Schlumberger array at AB/2 = 1000 ft.*

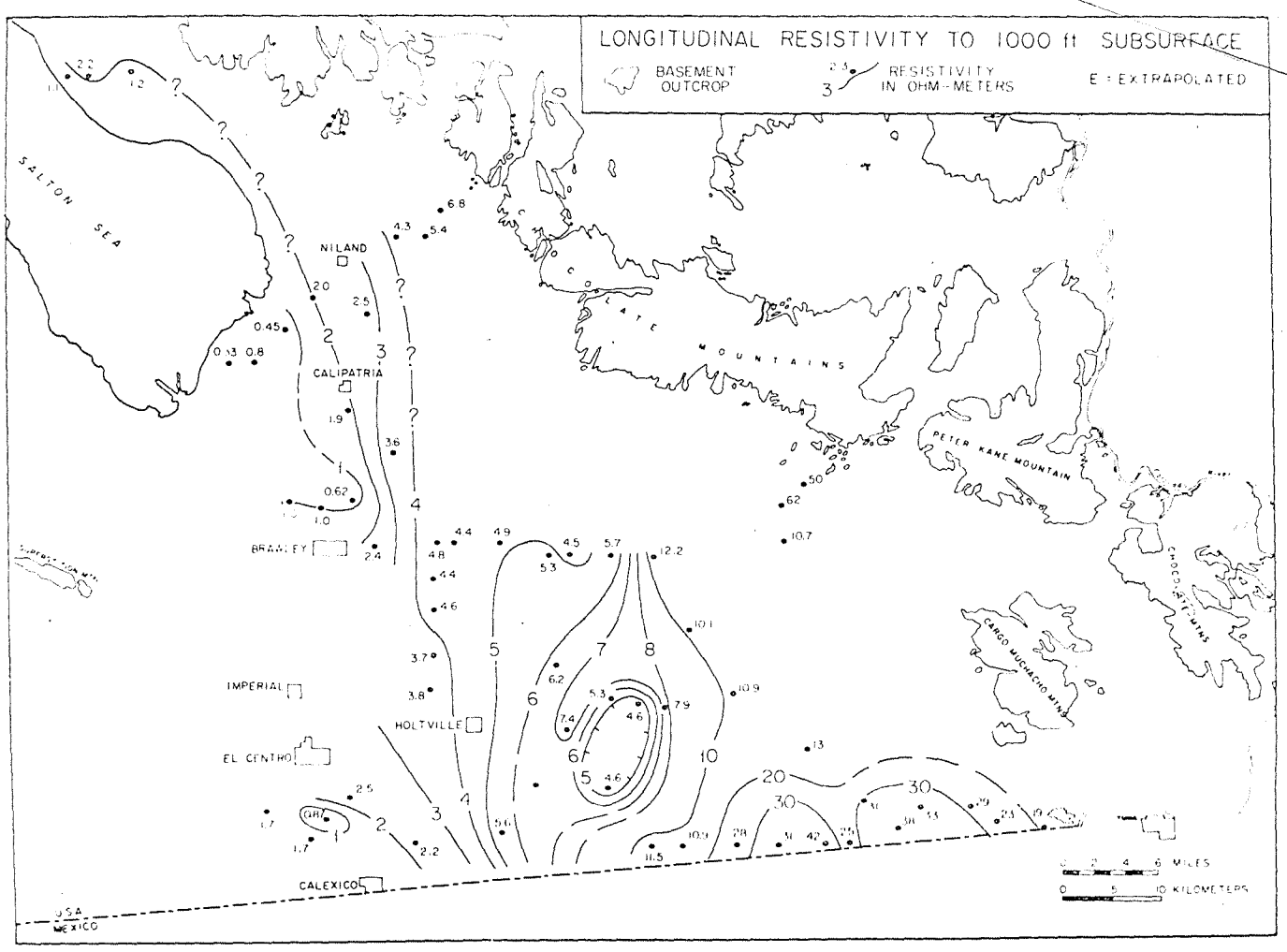

FIG. 5. — *Longitudinal-resistivity map computed from interpreted resistivities and thicknesses to 1000 ft subsurface.*

state stabilization of the potential field across the potential electrodes. For the case of a conducting stratus, with conductance S, underlain by an insulator, VEDRINTSEV (1963, p. 166-167) gives the current formation time t_c for the Schlumberger array as

$$t_c = 1.98\, S\, \frac{AB}{2} \text{ seconds} \qquad (4)$$

where

S = longitudinal conductance in mhos
AB = Schlumberger current electrode spacing in meters.

A third factor which occasionally added to errors of measurement was coupling between current and potential lines. Coupling causes an erroneous increase in the apparent resistivity.

A simple empirical test was devised in the course of this study to determine the reliability of a measurement. Readings were taken at more than one commutation rate at a given electrode spacing. The effect of all three factors was found (analytically or empirically) to increase the apparent potential difference between the potential electrodes if the commutation frequency was too high. Hence, a difference in potential electrode voltage of more than 3-5% between two commutation frequencies was used to judge the quality of the data. The data obtained with longer periods was deemed more reliable. Maximum AB/2 distances of 3000 to 8000 ft were achieved at most stations. The depth soundings for one of the profiles to be discussed are shown in Figure 3.

The depth soundings were interpreted initially by the auxiliary point method (ZOHDY 1965; ORELLANA and MOONEY 1966) and then by a computer-generated model. The program computes theoretical sounding curves for the Schlumberger array over a multi-layered horizontal earth and was produced by the Geophysical Institute of Israel by a Fortran conversion of an Algol program by ARGELO (1967). The interpretation was modified, when necessary, to obtain a reasonable fit between the field data and the computer-generated model (Figure 3). The plotted points on the depth soundings represent the field data, and the solid lines represent the computer-drawn and calculated interpretations.

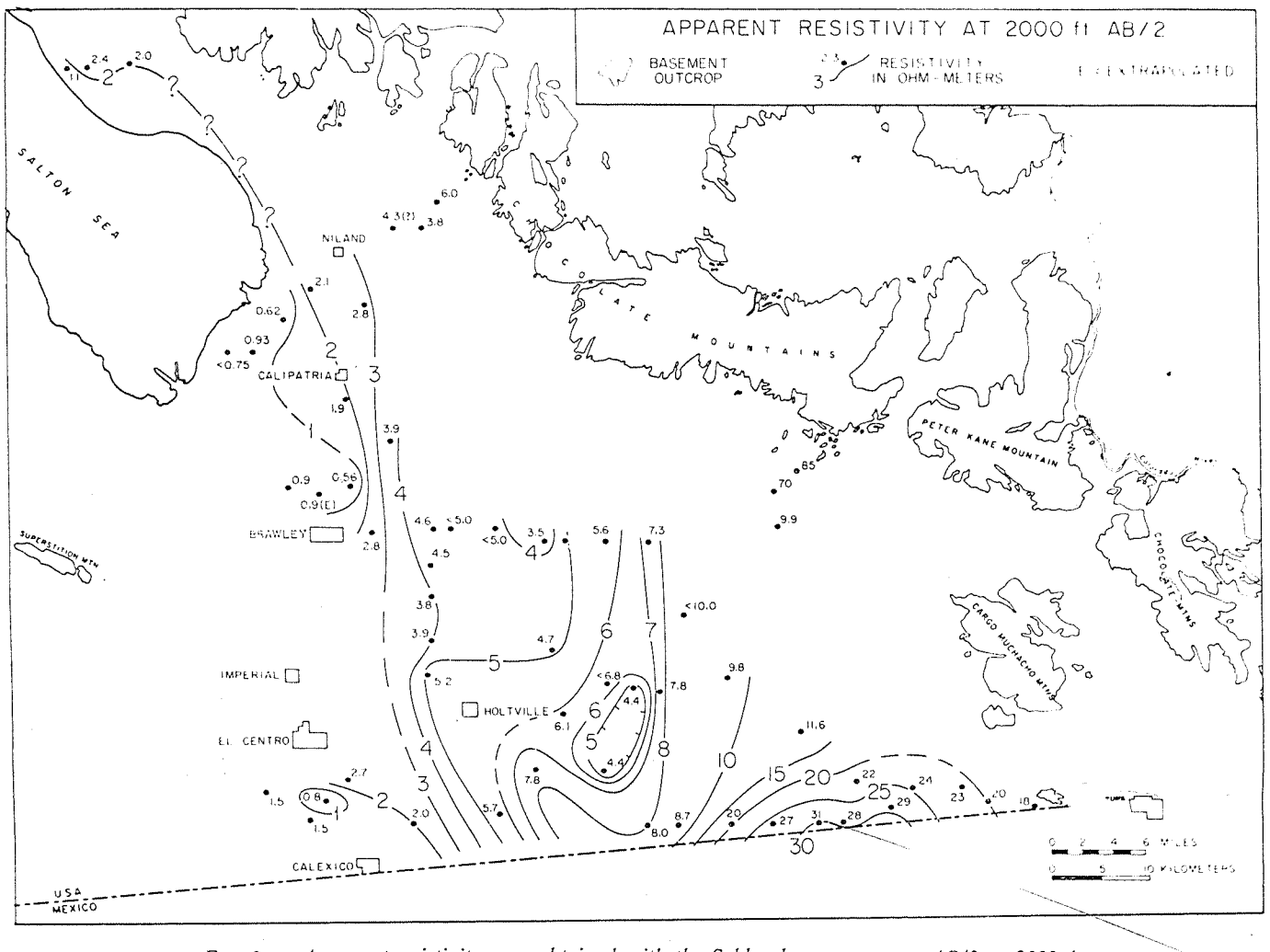

FIG. 6. — *Apparent-resistivity map obtained with the Schlumberger array at AB/2 = 2000 ft.*

Discussion of the resistivity study

GENERAL

A total of 59 resistivity depth soundings were made in the 1968-1970 field seasons (Figure 2). The correlation between gravity and temperature-gradient anomalies (MEIDAV and REX 1970, BIEHLER and COMBS 1972) was used to locate many of the stations. Results of the data analysis are presented in the form of iso-resistivity contour maps (Figures 4-9) and geoelectric cross-sections (Figures 10-13). The major findings of the resistivity study are:

1. A regional resistivity gradient exists in the Imperial Valley. Resistivities decrease gradually northwestward from the southeast corner of the Imperial Valley, near the present course of the Colorado River, to values about two orders of magnitude lower at the Salton Sea. This effect is clearly seen on all of the iso-resistivity maps (Figures 4-9). This resistivity gradient is believed to reflect primarily the increase in salinity of groundwater with increasing distance from the Colorado River. This interpretation is supported by detailed analysis, discussed below, of electrical borehole logs.

2. An abrupt drop in resistivity occurs at or near the Imperial fault in the southern part of the Imperial Valley. This abrupt change in resistivity, with much lower resistivities to the west, reflects primarily an abrupt change of salinity across the Imperial fault. This interpretation is supported by PAREDES's (personal communication) iso-salinity contour map of the Mexicali Valley. PAREDES shows that salinity gradually increases westward from about 500 ppm TDS (total dissolved solids) near the Colorado River at the U.S.-Mexican border, to more than 5000 ppm west of Mexicali, with a rather steep salinity gradient between Mexicali and where the fault crosses the border. Data collected by MARSHALL REED (University of California, Riverside, personal communication) show that an overwhelming majority of potable water wells in the Valley is located east of the Imperial fault. Scanty data suggest that salinity in shallow wells west of the Imperial fault is

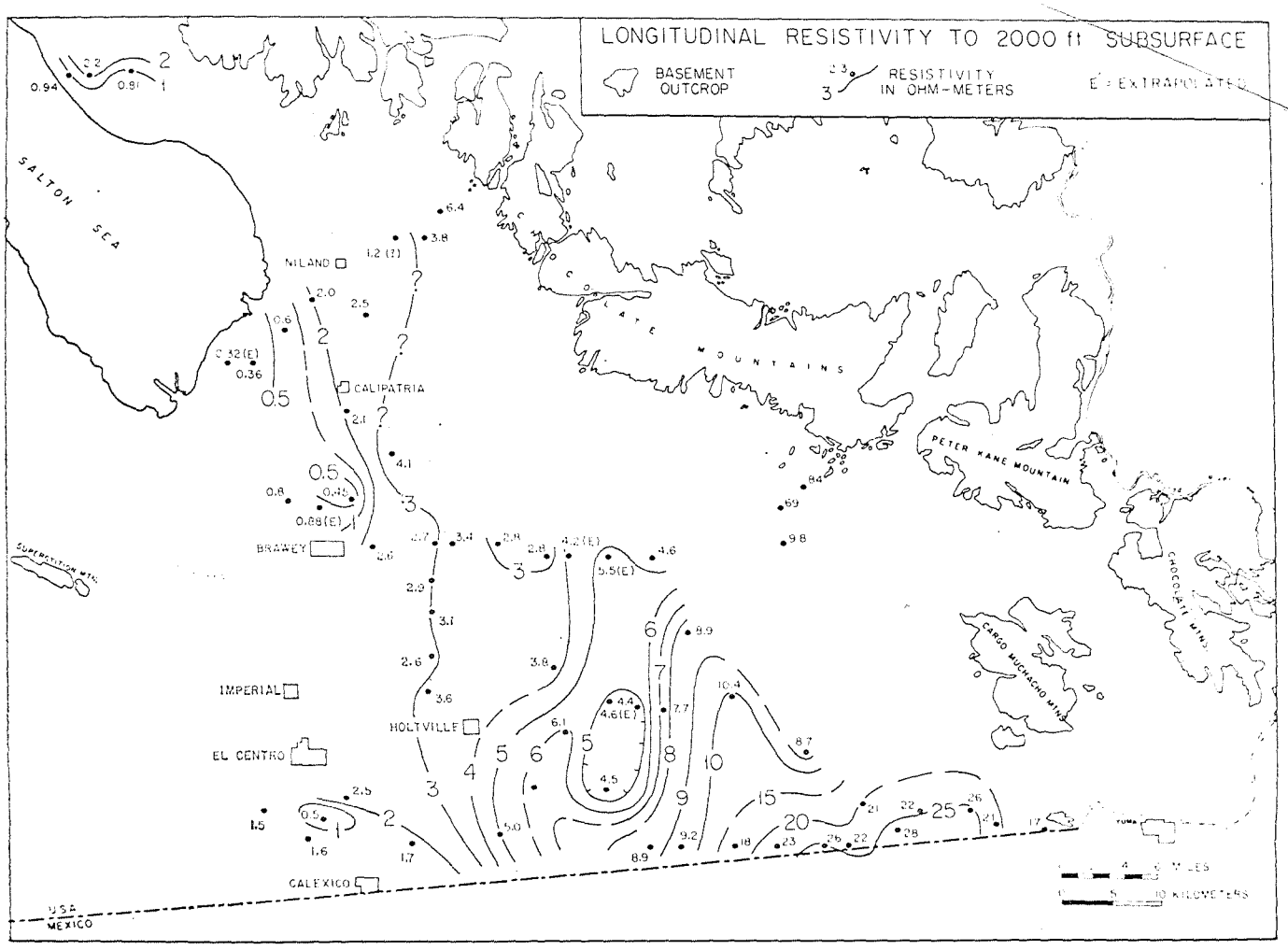

FIG. 7. — *Longitudinal-resistivity map computed from interpreted resistivities and thicknesses to 2000 ft subsurface.*

on the order of 8000 ppm TDS. This conforms to the picture obtained in the Mexicali Valley, just south of the border.

3. Local geothermal anomalies introduce a local decrease in resistivity. This is clearly seen to be the case for the North Brawley, Salton Sea Buttes, and East Mesa anomalies, named in Figure 2.

4. A number of acquicludes and aquitards exist, as reflected by abrupt or steeper-gradient changes in the resistivity cross-sections. In the more ambiguous cases, data from infrared photography, surface geology, hydrogeology, gravity, and magnetics, were utilized to support the interpretation.

ISO-RESISTIVITY CONTOUR MAPS

Both iso-apparent-resistivity and isolongitudinal-resistivity contour maps were constructed. When there is not a great variation between the resistivity of near-surface layers and the deeper layers, or when the thickness of the surface layer is small compared with the electrode spacing, both presentations are similar in appearance. If either condition is not met, the apparent-resistivity maps may show false anomalies, suggesting the existence of low-resistivity areas at depth where a thick low-resistivity surface layer exists. Conversely, the apparent-resistivity map may falsely suggest the existence of a high-resistivity area at depth where a thick high-resistivity surface layer exists. Because the resistivity survey was conducted over a terrain of highly varying near-surface resistivities, the longitudinal-resistivity maps, although not greatly different in appearance from the apparent-resistivity maps in this area, are deemed to be more reliable. In the study area surface-layer resistivities varied between about 5 ohm-m for the irrigation loams in the center of the valley to more than 1000 ohm-m for the sand dune areas.

Longitudinal resistivity is defined by ρ_L

$$\rho_L = \frac{\Sigma h_i}{\Sigma (h_i/\rho_i)} \qquad (5)$$

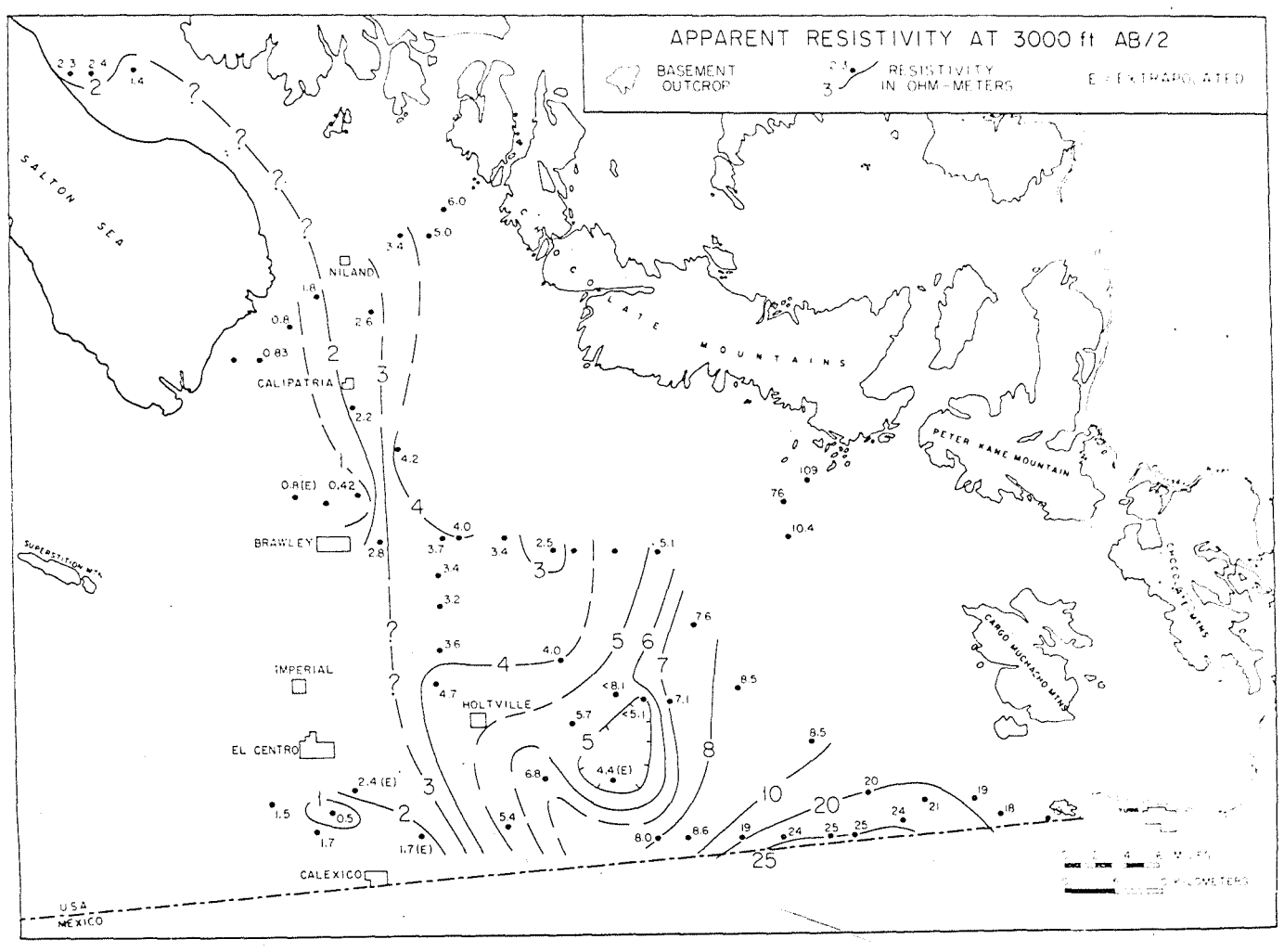

FIG. 8. — *Apparent-resistivity map obtained with the Schlumberger array at AB/2 = 3000 ft.*

where

h_i = thickness of i^{th} layer
ρ_i = true resistivity of the i^{th} layer.

The « true resistivity » and thickness of the individual layers were determined by the graphical and computer-assisted curve-matching techniques discussed earlier. Physically, longitudinal resistivity can be interpreted as the composite resistivity of resistors of finite thickness, connected in parallel. Visually, it may be conceived as the resistivity of a section of rocks if they were to be placed between two parallel plates extending to the depth of interest (in our case to 1000 ft, 2000 ft, and 3000 ft). Because it is necessary to have layer thicknesses and resistivities for the computation of longitudinal resistivity, such maps as shown in Figures 5, 7, and 9 can be prepared only when a full depth sounding curve is available.

Comparison of the apparent-resistivity and the longitudinal-resistivity maps resulted in the following conclusions:

1. The major features, such as the regional decrease in resistivity northward or the position of the Buttes anomaly, are readily discernible on both types of maps.

2. At 3000 ft probing depth, both maps are nearly identical.

3. At 2000 ft probing depth, both maps are fairly similar with the following exception. Although the data are sparse, the 2000 ft longitudinal-resistivity map suggests a resistivity decrease along the western front of the Sand Hills, which may be associated with the inferred fault along that front. Faulting associated with a resistivity drop often indicates favorable geothermal conditions. Hence, additional resistivity and temperature-gradient work should be conducted in that area.

4. At 1000 ft probing depth, the apparent-resistivity map is significantly different from the longitudinal-resistivity map. The East Mesa anomaly, east of Holt-

(5)

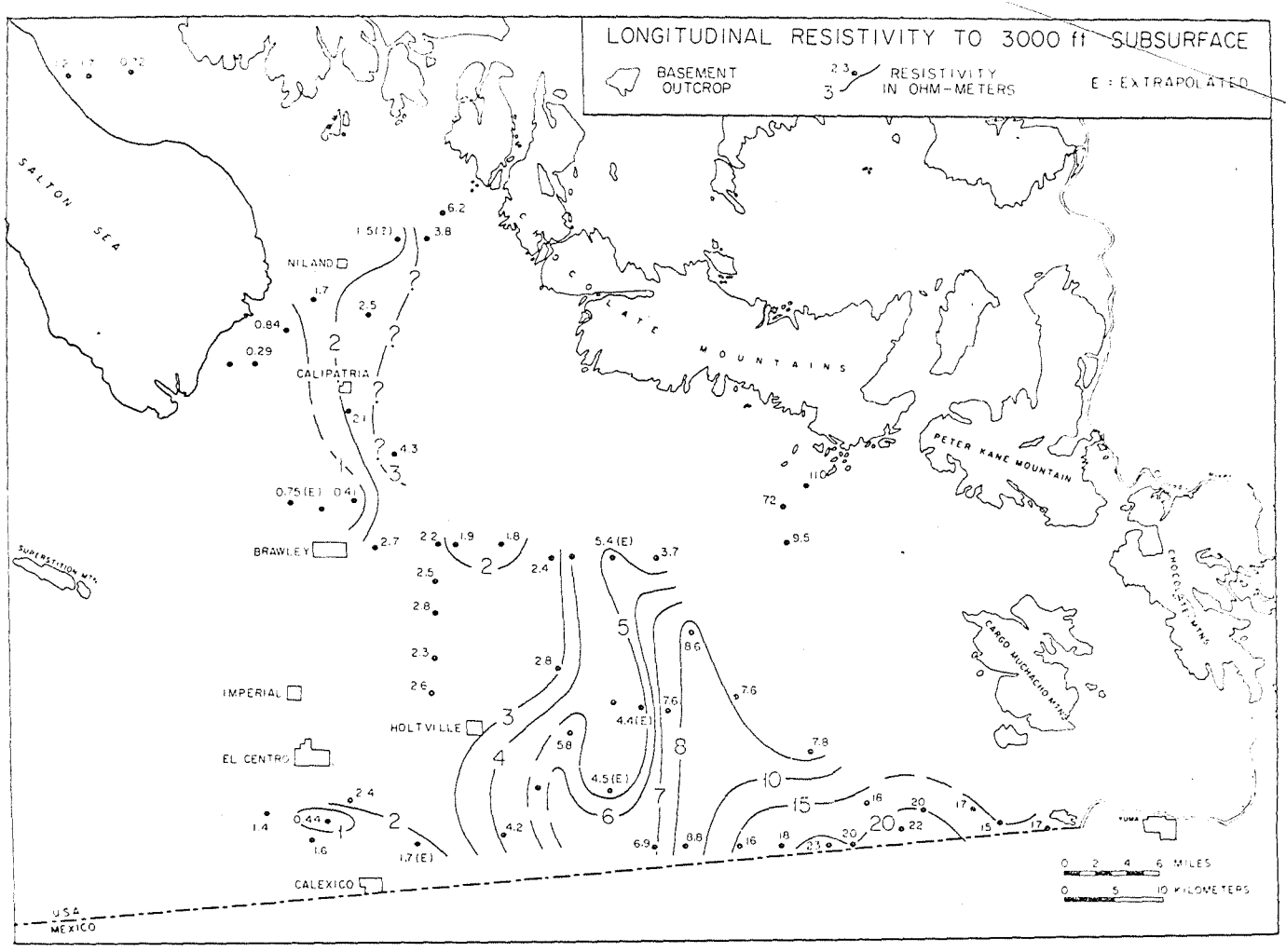

FIG. 9. — *Longitudinal-resistivity map computed from interpreted resistivities and thicknesses to 3000 ft subsurface.*

ville, appears considerably smaller on the apparent-resistivity map than on the longitudinal-resistivity map. Comparison with the temperature-gradient map by REX (1971) shows greater consistency with the longitudinal-resistivity map. The size of the anomaly, about 18 square miles within the 5 ohm-m contour lines, suggests that this area should be further studied. The complete Bouguer gravity map by BIEHLER (1964), which shows a positive anomaly over East Mesa, is consistent with the longitudinal-resistivity anomaly.

The longitudinal- and apparent-resistivity maps suggest that the Heber anomaly is of a very local nature. A very low longitudinal resistivity was determined at the center of the anomaly, 0.5 ohm-m at 2000 ft as compared with an average regional of about 2.5 ohm-m west of the Imperial fault. This suggests a high temperature anomaly at Heber, although of restricted areal dimensions. The steep horizontal gradient of the temperature-gradient map (REX 1971) is interpreted using half-width formulas for thermal anomalies (SIMMONS 1967) to indicate a very shallow source. This is believed to indicate either a narrow plume of thermal water which has risen to near-surface along a fault, or effect of interformation leakage due to uncontrolled drilling in the Amerada Petroleum Corporation Timkin No. 1 well.

The operational conclusion from the comparisons conducted between apparent- and longitudinal-resistivity maps is that for a 3000 ft effective probing depth, the apparent-resistivity map yields nearly as much information as the longitudinal-resistivity map, under the geological conditions of the Imperial Valley. The significance of this conclusion is that in any future work in the Valley, continuous profiling at 3000 ft spacing can be conducted rapidly to yield diagnostic data as to the major resistivity features which are related to geothermal gradient anomalies. Continuous profiling with a single electrode spacing can be conducted quickly and efficiently at a fraction of the cost of depth soundings. In areas other than the Imperial Valley, it may be necessary to conduct some depth soundings to establish the validity and optimal electrode spacing for continuous profiling.

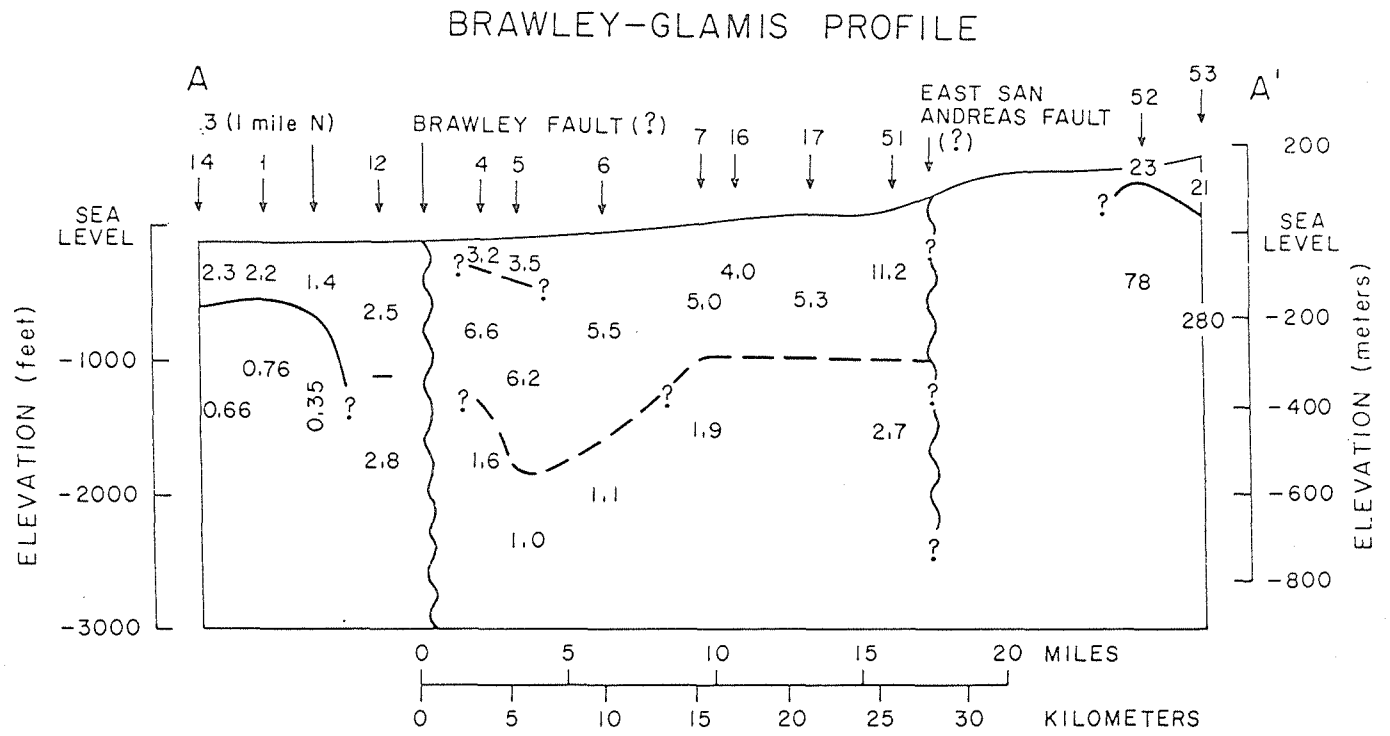

FIG. 10. — *Brawley-Glamis geoelectric cross-section (AA').*

GEOELECTRIC CROSS SECTIONS

Section A-A' (Figures 2 and 10). This cross-section runs from slightly west of Brawley to east of Sand Hills. The very low resistivity of 6.6 ohm-m or less, which is characteristic of the entire section west of Station 51, is typical of the northern half of the Imperial Valley. The increase in salinity combined with the high sediment porosity together produce resistivities of 2.8 ohm-m or less at depths greater than 1800 ft, even where the temperature-gradient map suggests a mild gradient of 4-7 °F/100 ft. The north Brawley thermal anomaly (stations 14, 1, 3) is, however, clearly identifiable, by virtue of the very low resistivity of 0.35-0.76 ohm-m at depths greater than 600 ft. This four-fold decrease in resistivity relative to surrounding rocks would require an eight-fold increase in temperature gradient were salinity and stratigraphic factors to be ignored. Compelling evidence suggests the existence of at least one, and perphaps two hydrologic discontinuities between the Sand Hills and the west end of the section, which could signify faults and would account for salinity and/or stratigraphic changes along the line. The discontinuity between stations 12 and 4 is believed to signify a fault.

Insufficient work has been done by us to assess the significance of these discontinuities on a regional scale. However, since favorable geothermal reservoir conditions are often associated with faulting, it would be of value to investigate the extent and significance of these features.

Stations 52 and 53 are located east of the Sand Hills. Both of these soundings suggest a bedrock depth less than 500 ft whereas station 51, just west of the Sand Hills, indicates a bedrock depth greater than 8000 ft. A fault or a series of faults may be assumed to cause the depth difference. This interpretation is supported by gravity and magnetic data.

Section B-B' (Figure 11). This is a N-S cross-section from Brawley to south of Heber, and shows clearly differences in resistivity of rocks on the two sides of the Imperial fault. At a depth of 1000 ft, the resistivity drops from 9-12 ohm-m northeast of the fault to about 2.4 ohm-m southwest of it. This change is attributed largely to the increase in salinity of groundwater west of the Imperial fault. Hydrological data by PAREDES show that west of Mexicali groundwater salinities are on the order of 2000-10,000 ppm NaCl. The fault probably behaves as an impermeable barrier to prevent or seriously retard the underground westward flow of fresh groundwater from the Colorado River into the brackish water west of the fault. The very low, very local resistivity anomaly associated with Heber (station 66) is interpreted as being associated with a very shallow hot body. The continuity of the intermediate-depth resistivity layer (9-12 ohm-m) between stations 4 and 11 is believed to denote a lower-salinity confined aquifer sandwiched between two higher-salinity layers.

Section C-C' (Figure 12). Station 28-30 were run across the San Andreas fault on the Durmid anticline, just east of the Salton Sea. The section clearly shows the effect of the San Andreas fault and suggests that

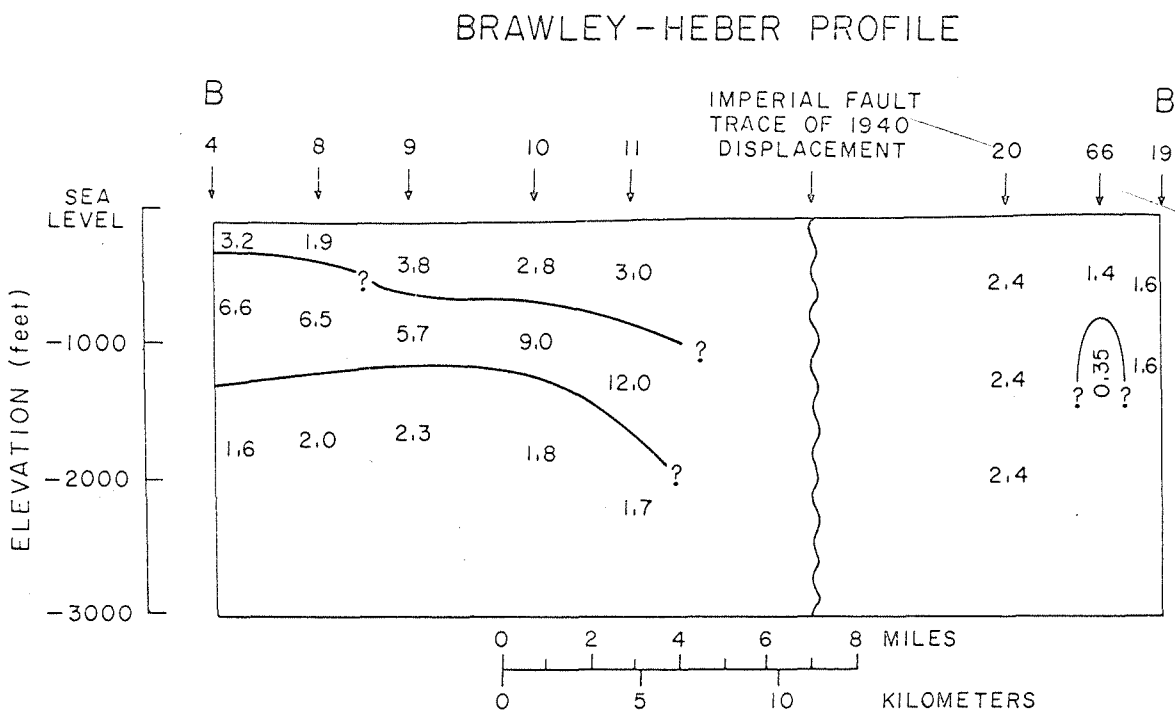

FIG. 11. — *Brawley-Heber geoelectric cross-section (BB').*

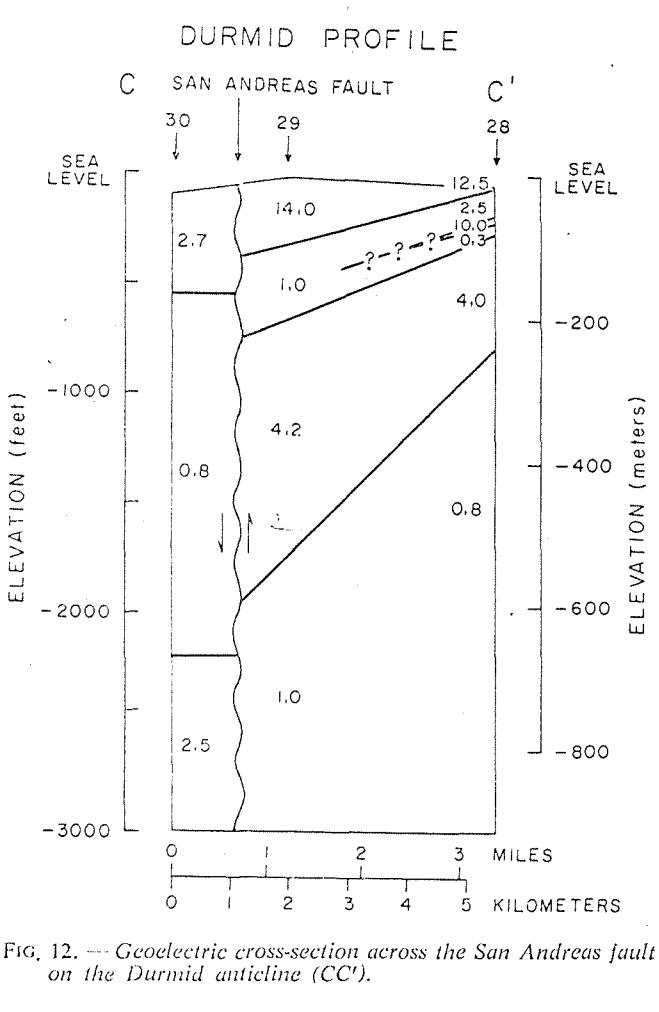

FIG. 12. — *Geoelectric cross-section across the San Andreas fault on the Durmid anticline (CC').*

the shallow strata west of the fault are more saline than east of the fault.

Section D-D' (Figure 13). This cross-section, near the U.S.-Mexico border shows that resistivity at any particular depth decreased gently westward to the Imperial fault, and more abruptly across that fault. The gradual decrease in resistivity westward, from about 20-24 ohm-m at 2000 ft depth near the Colorado River, to 3 ohm-m at that depth just east of the Imperial fault, probably reflects the change in salinity of the groundwater. The higher resistivities of 20-24 ohm-m near the Colorado River are typical of potable water in shaly sands. The observation that this fairly high resistivity extends to a depth of nearly half a mile for a distance of several miles away from the river is quite significant with regard to potential geothermal resources development in that area. It suggests that if a promising geothermal target should be encountered in that part of the Sand Hills which was studied by resistivity, it is likely to be characterized by low-salinity water. Hence, the corrosion and salinity problems which were met in the attempted development of the Salton Sea field, where salinities on the order of 33 percent were encountered, are not expected to arise in the southeastern portion of the Imperial Valley.

This conclusion may be further generalized by examination of the longitudinal-resistivity maps, geoelectric cross-sections, and the individual soundings to about one mile depth in the Holtville-Glamis-Yuma triangle. This area is characterized by a relatively low

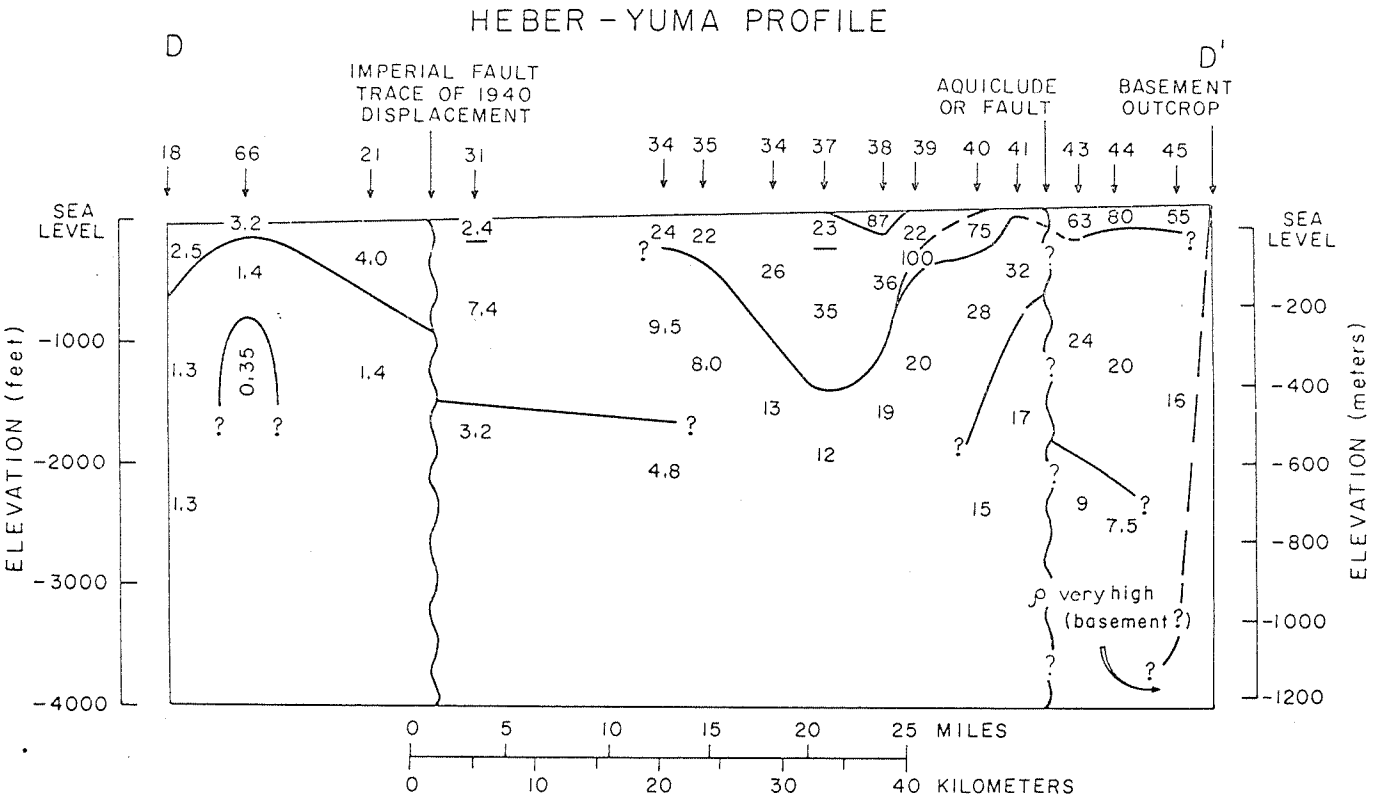

FIG. 13. — *Heber-Yuma geoelectric cross-section (DD').*

salinity, as distinct from the rest of the Valley. It may be further deduced that within the above triangle, the quality of the groundwater probably improves as the Yuma apex is approached.

Salinity and porosity in the Imperial Valley

SALINITY COMPUTATIONS

Analysis of a limited number of geophysical borehole logs obtained in the course of petroleum and geothermal exploration provides an insight into the salinities and porosities of the sediments of the Imperial Valley. Only three well logs have been analyzed to date, hence the interpretation given below is tentative. The logs employed are those of the Standard Wilson No. 1, American Petrofina Salton Trough 27-1, and Shell State of California No. 1 (Figure 2).

WYLLIE (1963) gives the resistivity of the formation water, R_w, in ohm-m as

$$R_w = \frac{R_{mf}}{\log^{-1}\,(SP/(60+0.133T))} \qquad (6)$$

where

SP = self potential obtained from the SP log in millivolts
T = temperature in degrees Fahrenheit
R_{mf} = resistivity of mud filtrate in ohm-m.

The formation factor F was determined from

$$F = R_o/R_w \qquad (7)$$

R_o was determined from the induction log or the long normal log. Figure 14 is a plot of the apparent formation factor as a function of depth for the three wells. The apparent formation factor differs from formation factor in that it includes the solid-conductivity effect of clay. The effect of clay entrained in the sediments is to lower the formation factor. It is likely that the effect of clay on the overall resistivity, and hence the change it affects in the formation factor, is greater at shallow depths. The plot in Figure 14 suggests that a major difference exists in the characteristics of the sediments in the Salton Sea field (Shell No. 1) as compared with the sediments of the Wilson No. 1 and the American Petrofina well.

In the two latter wells, the apparent formation factor increases gradually from about 4 at shallow depth to about 50 ± 10 at 9000 ft. In the Shell No. 1, on the other hand, the apparent formation factor increases to 130 at 4400 ft. This steep increase at the Salton Sea field suggests a very rapid decrease in interconnected porosity at that well, perhaps due to self-sealing (FACCA 1967) or low-grade metamorphism.

The relationship between depth and formation factor provides a way of estimating the salinity in those areas where that relationship holds. The salinities calculated here are the maximal salinities, because the

effect of clay is ignored. Figure 15 was calculated using equation (1) and the resistivity-formation factor-salinity-temperature nomogram by MEIDAV (1970 a) for the case of a geothermal gradient of 5°F/100 ft, a surface temperature of 80°F, and a formation factor function as shown by the upper solid curve in Figure 14.

In the area south of Brawley and east of the Imperial fault, resistivities are greater than 3 ohm-m to a depth of several thousands of feet. Hence from Figure 15 salinities should be considerably less than 30,000 ppm NaCl equivalent. Along profile D-D', resistivities at a depth of about one mile are 10-20 ohm-m (stations 36-45). Hence, the salinities along that section and at that depth are likely to be considerably less than 7000 ppm.

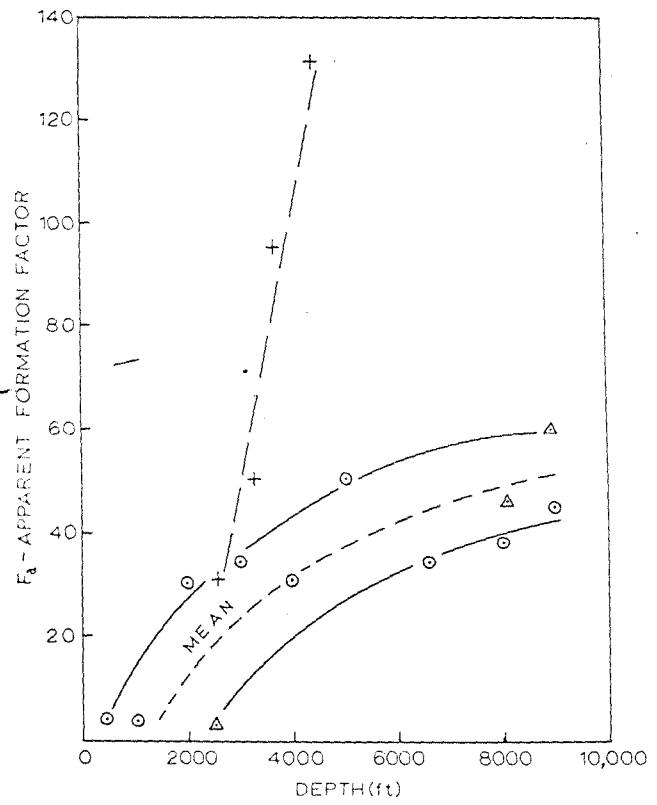

FIG. 14. — *Depth-formation factor relationships for three deep wells (⊙ Standard Wilson No. 1, + Shell State of California No. 1, and Δ American Petrofina Salton Trough 27-1).*

An appreciation of the drastic change in salinity from north to south, discussed earlier in conjunction with the regional resistivity gradient, can be obtained by also calculating salinity at the Shell No. 1 well, on the south shore of the Salton Sea. At a depth of 4000 ft, the apparent formation factor has been calculated as 100 from the electrical log. Stations 26 and 27, in the vicinity of that well, show that the bulk resistivities at that depth are on the order of 1.5 ohm-m. Assuming again a temperature gradient of 5°F/100 ft, a salinity of 170,000 ppm is obtained. This result agrees reasonably well with measurements of salinities on the order of 330,000 ppm near the Salton Sea field (MCNITT 1963). It will be necessary to determine the formation factor functions for all existing wells in the valley, to be combined with resistivity data obtained on the surface, before a full quantitative evaluation of the salinity of the valley is attempted.

POROSITY COMPUTATIONS

Porosities were intially computed from electrical logs using the modified Archie equation (1), assuming cementation exponents of 1.8 and 2.0. The porosities thus obtained were then employed to provide the under-compaction correction factor for the Wyllie time-average equation, modified by TIXIER ET AL. (1968).

$$\Phi_c = \frac{\Delta t - A t_{ma}}{\Delta t_f - \Delta t_{ma}} \cdot \frac{1}{C_p} \qquad (8)$$

where

Φ_c = porosity corrected for low apparent matrix velocity
Δt = observed transit time, milliseconds/ft
Δt_{ma} = matrix transit time, assumed to be 15,700 ft/second
Δt_f = fluid transit time, 5300 ft/second
C_p = under-compaction correction factor.

A number of procedures have been proposed for empirically establishing the correction factor (e.g., TIXIER ET AL. 1959 and 1968). In this study, we have determined C_p, the under-compaction correction factor, by assuming a reasonable matrix transit time and divi-

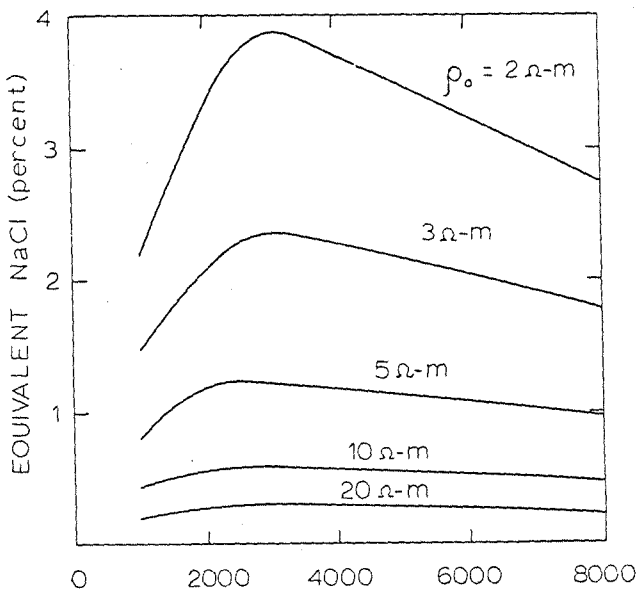

FIG. 15. — *Calculated salinity at different depths for varying rock resistivities. The geothermal gradient has been taken as 5°F/100 ft, the surface temperature as 80°F, and the formation factor function as the upper solid curve in Figure 14.*

ding the uncorrected porosity by the porosity obtained from the electric log in predominantly sandy formations. The electric log porosity was obtained from equation (1), where m, the cementation factor, was assumed to be 1.8 and 2.0. Studies by well log analysts (SCHLUMBERGER 1969 a, b) show that the cementation factor for poorly compacted strata should fall between the above values.

Porosities were thus calculated for the following wells: Western Geothermal Sinclair No. 3, Standard Wilson No. 1, and American Petrofina Salton Trough 27-1. Of these wells, only Sinclair No. 3 showed a consistent correction factor for the various depths. Figure 16 shows the generalized velocity log for that well with

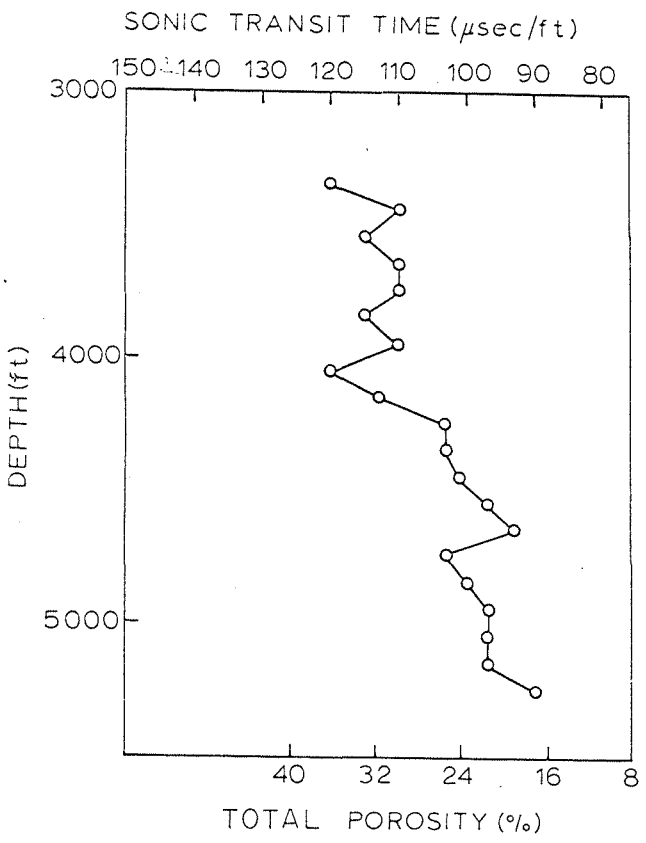

FIG. 16. — *Sonic velocity-porosity relationships for the Western Geothermal Sinclair No. 3 well. Porosity correction for undercompaction was derived from electrical log data (v_{matrix} = 15,000 ft/sec, v_{liquid} = 5300 ft/sec).*

the porosity corrected for under-compaction. Porosity on the order of 22 percent at a depth of about one mile at that well, along with similar results obtained for partially analyzed wells, suggests that drilling for geothermal fluids can be carried out to a depth greater than one mile with the expectation of encountering sufficient porosities in much of the area. This conclusion is not valid unless the specific yield (effective porosity) is shown to be a substantial portion of the total porosity which is plotted in Figure 16. Specific yield (or effective porosity) is interconnected porosity. BEAN (in press) gives relationships between rock type and specific yield for near-surface conditions and lists the average specific yield of clay as only one percent, although its total porosity may be as high as 50 percent. Thus, total porosity is probably of use in estimating specific yield only for essentially sandy sections of logs.

The analysis presented above must be refined by including the data from the Cerro Prieto field and the remaining petroleum prospect wells in the Imperial Valley. The calculated parameters should be corrected, wherever possible, by comparison with actual porosities and salinities obtained in the course of drilling. However, by combining data from a small number of geologically and geophysically logged wells with geophysical data on the surface, it is possible to make a reasonable approximation of the regional variations of salinity and porosity.

Conclusions

The electrical resistivity survey which was conducted in 1968 and 1970 resulted in the following major conclusions:

1. A regional salinity gradient exists in the Imperial Valley, trending northwest. The regional salinity is lowest near the Colorado River at Yuma and gradually increases northwestward towards the Salton Sea. The salinity gradient is in the same direction as the regional groundwater gradient east of the Imperial fault.

2. Nearly fresh or slightly brackish water exists in the sediments of the Imperial Valley, from Yuma to about 15 miles west of the Sand Hills, along the Mexican border. The thickness of this non-saline layer extends to 0.5 miles depth in the Sand Hills, along the Mexican border. The relatively high resistivities obtained to the maximal probing depth of 8000 ft suggest that salinities are quite low to that depth.

3. The Imperial fault behaves as an aquiclude south of El Centro with expected groundwater salinities much greater west of it, perhaps by and order of magnitude, relative to those east of the fault. A few lesser aquicludes or aquitards exist in the valley.

4. A combination of ground resistivity data with geophysical borehole logs, permits semi-quantitative estimates of the salinity and porosity variation throughout the valley. While incomplete as yet, the analysis suggests that the Imperial Valley sediments are undercompacted on the whole, and hence possess relatively high porosities to great depths. An exception to this generalization may exist at the Salton Sea geothermal field itself, where low-grade metamorphism may have affected the physical characteristics of the sediments (WHITE 1963). It is believed, based upon the ground resistivity data, that the area between Holtville, Brawley,

and Yuma is characterized by low levels of salinity, varying between semi-fresh (less than 1000 ppm) and brackish—but at least one order of magnitude less saline than the Salton Sea field.

5. The East Mesa resistivity low, which is associated with a temperature-gradient high and a gravity high is considered a prime target of further exploration. Although the temperature gradients in that area (7-10 °F/100 ft) are not exceptionally high when compared with other geothermal areas of the world, the high porosity to great depths makes it feasible to consider deep drilling in that area.

6. Operationally, it has been shown that a much quicker coverage of terrain can be accomplished by carrying out continuous profiling at a large constant electrode separation.

Acknowledgements

This study was conducted at the Institute of Geophysics and Planetary Physics, University of California, Riverside, California, under funding from the National Science Foundation, the U. S. Bureau of Reclamation, the Chevron Oil Field Research Company, and the University of California Intramural Fund. Our thanks to Drs. SHAWN BIEHLER, LEWIS COHEN, JIM COMBS, and ROBERT REX, and to Messrs. TOM GETTS and MARSHALL REED for their constructive reviews.

REFERENCES

ARGELO S. M. 1967 — Two computer programs for the calculation of standard graphs for resistivity prospecting. *Geophysical Prospecting*, v. 15, 1, *71.*

BABCOCK E. A. 1969 — Structural geology and geophysics of the Durmid area, Imperial Valley, California.*University of California, Riverside, California, Ph. D. thesis, 145 p.*

BEAN R. *in press.* — Groundwater storage and artificial recharge. *New York, United Nations.*

BIEHLER S. 1964 — Geophysical study of the Salton trough of southern California. *California Institute of Technology, Pasadena, California, Ph. D. thesis, 139 p.*

BIEHLER S., COMBS J. 1972 — Correlation of gravity and geothermal anomalies in the Imperial Valley, southern California (abstr.). *Geol. Soc. Amer (Cordilleran Section), Honolulu, Hawaii Program.*

BIEHLER S., KOVACH R. L., ALLEN C. R. 1964 — Geophysical framework of the northern end of the Gulf of California structural province *in van Andel T. H. and Shor G. G. Jr., eds., Marine Geology of the Gulf of California - a symposium. Am. Assoc. Petr. Geol. Mem.* 3, *126.*

BREUSSE J. J. 1961 — Contribution des methodes geophysiques a la prospection des champs geothermiques. *Proceedings of U.N. Conference on New Sources of Energy, Rome, 141.*

COMBS J. 1971 — Heat flow and geothermal resource estimates for the Imperial Valley *in Rex R. W., principal investigator, Cooperative geological-geophysical-geochemical investigation of geothermal resources in the Imperial Valley of California. Institute of Geophysics and Planetary Physics, Univ. of California, Riverside, 5.*

DAKHNOV V. N. 1962 — Geophysical well logging. *Translated by G. V. Keller. Quart. of Col. School of Mines,* v. 57, 2, *445.*

DIBBLE T. W., Jr., 1954 — Geology of the Imperial Valley Region, California. *Calif. Div. of Mines Bull.* 170, *21.*

FACCA G., TONANI F. 1967 — The self sealing geothermal field. *Bull. Volcan.*, v. 30, *271.*

GRISCOM A., MUFFLER L. J. P. 1971 — Aeromagnetic map and discussion of the Salton Sea geothermal area California. *U. S. Geol. Survey Geophys. Inv. Map GP-754.*

HAYAKAWA M. 1966 — Geophysical study of Matsukawa geothermal area, Iwate Prefecture, Japan. *Bull. Volcan.*, v. 29, *499.*

ISACKS B., OLIVER J., SYKES L. 1968 — Seismology and the new global tectonics. *J. Geophys. Res.*, v. 73, 5855.

KELLER G. V., FRISCHKNECHT F. C. 1966 — Electrical methods in geophysical prospecting. *New York, Pergamon Press, 517 p.*

KOENIG J. B. 1967 — The Salton-Mexicali geothermal province, *Cal. Div. Mines Geol., Mineral Information Service*, v. 20, 7, *75.*

MCNITT J. R. 1963 — Exploration and development of geothermal power in California. *Cal. Div. Mines Geol. Spec. Report 76, 45 p.*

MEIDAV T. 1970 a — Application of electrical resistivity and gravimetry in deep geothermal exploration *in Proceedings of the United Nation Symposium on the Development and Utilization of Geothermal Resources, Pisa 1970. Geothermics*, sp. issue 2.

MEIDAV T. 1970 b — Arrays and nomograms for electrical resistivity exploration. *Geophys. Prospecting*, v. 18, 4, *550.*

MEIDAV T., REX R. W. 1970 — Investigation of geothermal resources in the Imperial Valley and their potential value for desalination of water and electricity production. *Preliminary report, Institute of Geophysics and Planetary Physics, Univ. of California, Riverside, 54 p.*

MENARD H. W. 1960 — The East Pacific Rise, *Science*, v. 132, *1737.*

ORELLANA E., MOONEY H. M. 1966 — Master tables and curves for vertical electrical sounding over layered structures. *Madrid, Interciencia.*

REX R. W. 1971 — Geothermal resources in the Imperial Valley *in D. Seckler ed., California water — a study in resource management. Berkeley, University of California Press, 190.*

REX R. W. ET AL. 1971 — Cooperative geological-geophysical-geochemical investigations of geothermal resources in the Imperial Valley of California. *Institute of Geophysics and Planetary Physics, Univ. of California, Riverside, 153 p.*

SCHLUMBERGER 1969 a — Log interpretation principles. *New York, Schlumberger Ltd.*

SCHLUMBERGER 1969 b — Log interpretation charts. *New York, Schlumberger Ltd.*

SIMMONS G. 1967 — Interpretation of heat flow anomalies. *Rev. of Geophysics*, v. 5, *43.*

STACEY F. D. 1969 — Physics of the earth. *New York, Wiley, 324 p.*

STUDT F. E. 1958 — Geophysical reconnaissance at Kawerau, New Zealand. *N. Z. Jour. of Geology and Geophysics*, v. 1, 2, *219.*

TIXIER M. P., ALGER R. P., TANGUY D. R. 1959 — Sonic logging. *Jour. Pet. Technology*, v. 2, *5, 106.*

TIXIER M. P., MORRIS R. L., CONNEL J. G. 1968 — Log evaluation of low-resistivity pay sands in the Gulf Coast. *The Log Analyst*, v. 9, *3.*

VEDRINTSEV G. A. 1963 — Apparatus configuration for vertical electrical logging *in Handbook of Geophysics, A. G. Tarkhov, editor, Moscow, Gostoptekhizdat.*

WARD S. H., FRASER D. C. 1967 — Conduction of electricity in rocks *in Mining Geophysics*, v. 2. *Society of Exploration Geophysicists, 197.*

WHITE D. 1963 — Geothermal brine well. Mile deep drill hole may tap ore-bearing magnetic water and rocks undergoing metamorphism. *Science*, v. 139, *919.*

WYLLIE M. R. J. 1963 — The fundamentals of well log interpretation. *New York, Academic Press.*

ZOHDY A. 1965 — The auxiliary point method of electrical sounding and its relationship to the Dar Zarrouk parameters. *Geophysics*, v. 30, 4, *644.*